

Self-Supervised Learning by Cross-Modal Audio-Video Clustering

Humam Alwassel^{1*} Dhruv Mahajan² Lorenzo Torresani² Bernard Ghanem¹ Du Tran²

¹King Abdullah University of Science and Technology (KAUST) ²Facebook AI

{humam.alwassel,bernard.ghanem}@kaust.edu.sa {dhruvm,torresani,trandu}@fb.com

Abstract

The visual and audio modalities are highly correlated yet they contain different information. Their strong correlation makes it possible to predict the semantics of one from the other with good accuracy. Their intrinsic differences make cross-modal prediction a potentially more rewarding pretext task for self-supervised learning of video and audio representations compared to within-modality learning. Based on this intuition, we propose Cross-Modal Deep Clustering (XDC), a novel self-supervised method that leverages unsupervised clustering in one modality (e.g. audio) as a supervisory signal for the other modality (e.g. video). This cross-modal supervision helps XDC utilize the semantic correlation and the differences between the two modalities. Our experiments show that XDC significantly outperforms single-modality clustering and other multi-modal variants. Our XDC achieves state-of-the-art accuracy among self-supervised methods on several video and audio benchmarks including HMDB51, UCF101, ESC50, and DCASE. Most importantly, the video model pretrained with XDC significantly outperforms the same model pretrained with full-supervision on both ImageNet and Kinetics in action recognition on HMDB51 and UCF101. To the best of our knowledge, XDC is the first method to demonstrate that self-supervision outperforms large-scale full-supervision in representation learning for action recognition.

the location and timing of sounds is leveraged as an important cue by humans to direct our spatiotemporal visual attention [20, 43]. The influence of hearing sounds in visual perception is also suggested by studies showing that individuals affected by profound deafness exhibit poorer visual perceptual performance compared to age-matched hearing controls [11, 39].

In this work, we investigate the hypothesis that spatiotemporal models for action recognition can be reliably pretrained from *unlabeled* videos by capturing cross-modal information from audio and video. The motivation for our study stems from two fundamental challenges facing a fully-supervised line of attack to learning video models. The first challenge is the exorbitant cost of scaling up the size of manually-labeled video datasets. The recent creation of large-scale datasets for action recognition [4, 26, 27] has undoubtedly enabled a major leap forward in the accuracy of models for video understanding. However, it may be argued that additional significant gains by dataset growth may not be seen unless we scale up existing labeled datasets by several orders of magnitude. In the short term this may be difficult to achieve. The second challenge is posed by the unclear definition of suitable label spaces for action recognition. Recently introduced video datasets differ substantially in their label spaces, which range from object-independent actions [16] to sports [26] and verb-noun pairs representing activities in the kitchen [7]. This suggests that the definition of the “right” label space for action recognition, and more generally for video understanding, is still very much up for debate. It also implies that finetuning models pretrained on large-scale labeled datasets is a sub-optimal proxy for learning models for small- or medium-size datasets due to the label-space gap often encountered between source and target datasets.

In this paper, we present three different approaches for training video models from self-supervised audio-visual information. At a high-level, the idea behind all three frameworks is to leverage one modality (say, audio) as a supervisory signal for the other (say, video). We posit that this is a promising avenue because of the simultaneous synergy and complementarity of audio and video: correlations be-

1. Introduction

Do we need to explicitly name the actions of “laughing” or “sneezing” in order to recognize them? Or can we learn to visually classify them without labels by associating characteristic sounds with these actions? Indeed, a wide literature in perceptual studies provide evidence that humans rely heavily on hearing sounds to make sense of actions and dynamic events in the visual world. For example, objects moving together are perceived as bouncing off each other when the visual stimulus is accompanied by a brief sound [57] and

*Work done during an internship at Facebook AI

tween these two modalities make it possible to perform prediction from one input space to the other, while their intrinsic differences make cross-modal prediction an enriching self-supervised task compared to within-modality learning. More specifically, we adapt the single-modality DeepCluster work of Caron *et al.* [5] to our multi-modal setting. DeepCluster was introduced as a self-supervised procedure for learning general image representations. It alternates between unsupervised clustering of image features and using these cluster assignments as pseudo-labels to revise the image representation in order to yield better classification of images into clusters. In our work, the clusters learned from one modality are used as pseudo-labels to refine the representation for the other modality. In two of our approaches—Multi-Head Deep Clustering (MDC) and Concatenation Deep Clustering (CDC)—the pseudo-labels from the second modality are *supplementary*, *i.e.*, they complement the pseudo-labels generated on the first modality. The third approach—Cross-Modal Deep Clustering (XDC)—instead uses the pseudo-labels from the other modality as *exclusive* supervisory signal. This means that in XDC, the clusters learned from audio drive the learning of the video representation and, vice versa, video-based pseudo-labels are used to refine the audio representations. Our experiments provide support for several interesting conclusions:

- All three of our cross-modal deep clustering methods yield audio and video representations that generalize better to the downstream tasks of action recognition and audio classification, compared to their within-modality counterparts.
- XDC (*i.e.*, the cross-modal deep clustering relying on the other modality as an exclusive supervisory signal) outperforms all the other approaches. This underscores the complementarity of audio and video and the benefits of learning label-spaces across modalities.
- We demonstrate that self-supervised cross-modal learning with XDC on a large-scale video dataset yields an action recognition model that achieves higher accuracy when finetuned on HMDB51 or UCF101, compared to that produced by fully-supervised pretraining on Kinetics. To the best of our knowledge, this is the first method to demonstrate that self-supervised video representation learning outperforms large-scale fully-supervised pretraining for action recognition.

2. Related Work

Early unsupervised representation learning. Pioneering work in unsupervised learning of video models includes deep belief networks [21], autoencoders [22, 63], shift-invariant decoders [52], sparse coding algorithms [33], and stacked ISAs [32]. While these approaches learn by reconstructing the input, our approach focuses on learning from a self-supervised pretext task, in which we construct pseudo-

labels for supervised learning from the unlabeled data.

Self-supervised representation learning from images.

One line of pretext tasks exploits spatial context in images, *e.g.* by predicting the relative position of patches [8] or solving jigsaw puzzles [41]. Another line of work involves creating image classification pseudo-labels, *e.g.* through artificial rotations [13] or clustering features [5]. Other self-supervised tasks include colorization [74], inpainting [47], motion segmentation [46], and instance counting [42].

Self-supervised representation learning from video.

In recent years, several approaches have extended image pretext tasks to video [28, 68, 73]. Other pretext tasks for video modeling include temporal frame ordering [9, 34, 38, 72], establishing region or object correspondences across frames [23, 24, 69, 70], predicting flow [31] or colors [66], as well as tracking [71]. Moreover, a large set of self-supervised approaches on video are built upon the pretext task of future frame prediction [36, 37, 59, 64, 65]. Unlike this prior work, our self-supervised model makes use of two modalities, video and audio.

Cross-modal learning and distillation. Inspired by the human multi-modal sensory system [6, 40], researchers have explored learning using multiple modalities, *e.g.* video and audio. Here, we review the relevant work in this area and contrast these methods with our cross-modal deep clustering approach. Several approaches [2, 17] train with full supervision an encoder on one modality (*e.g.* RGB) and then use the pretrained encoder to transfer the discriminative knowledge to an encoder of a different modality (*e.g.* depth). Unlike these methods, our approach is purely self-supervised and does not require pretraining an encoder with full supervision. Other approaches learn from unlabeled multi-modal data for a specific target task, *e.g.* sound source localization [75] and audio-visual co-segmentation [54]. Instead our method aims at learning general visual and audio representations that transfer well to a wide range of downstream tasks. Previous cross-modal self-supervised representation learning methods most relevant to our work include audio-visual correspondence [1], audio-visual temporal synchronization [29, 44], and learning image representations using ambient sound [45]. While audio-visual correspondence [1, 45] uses only a single frame of a video, our method takes a video clip as an input. Temporal synchronization [29, 44] requires constructing positive/negative examples corresponding to in-sync and out-of-sync video-audio pairs. This sampling strategy makes these approaches more difficult to scale compared to ours, as many potential out-of-sync pairs can be generated, yielding largely different results depending on the sampling choice [29].

3. Technical Approach

In this section, we briefly discuss previous work on single-modality deep clustering in the image domain [5].

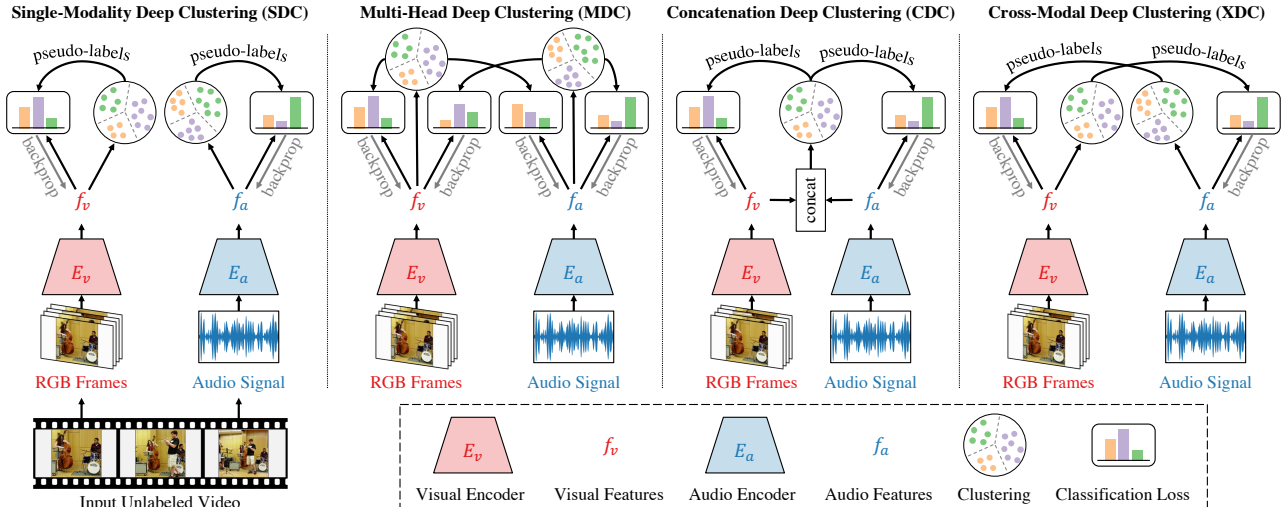


Figure 1: **Overview of our framework.** We present Single-Modality Deep Clustering (SDC) baseline vs. our three different proposed models: Multi-Head Deep Clustering (MDC), Concatenation Deep Clustering (CDC), and Cross-Modal Deep Clustering (XDC) for multi-modal deep clustering. Unlabeled videos are inputted into the video and audio encoders (E_v and E_a) to produce visual and audio features (f_v and f_a). These features, or the concatenation of them, are clustered using k -means. The cluster assignments are then used as pseudo-labels to train the two encoders. The process is started with randomly-initialized encoders, then alternates between clustering to generate pseudo-labels and training to improve the encoders. The four models employ different ways to cluster features and generate self-supervision signals for learning the visual and audio representations.

Then, we introduce our multi-modal deep clustering framework for representation learning, where we propose three different approaches. Finally, we address some optimization challenges and discuss differences with respect to single-modality deep clustering. Figure 1 provides an overview of our three approaches and contrasts them to the single-modality counterpart.

3.1. Single-Modality Deep Clustering

Caron *et al.* [5] introduced DeepCluster, a framework for self-supervised representation learning from images. DeepCluster iteratively clusters deep features from a single-modality encoder, and then uses the cluster assignments to train the same encoder to improve its representation. Inspired by the simplicity of this work, our paper studies deep clustering in the large-scale multi-modal setting. We expect the simplicity of the training will make our approaches much easier to scale, thus we can take advantages of large-scale pretraining, where we expect the self-supervision signal to be more useful and less-biased to data sampling. For completeness, we briefly summarize DeepCluster details.

Let X be the set of unlabeled inputs (*e.g.* images), E be a neural network encoder that maps an input $x \in X$ to a deep feature vector $f \in \mathbb{R}^d$. DeepCluster iteratively clusters the deep features $F = \{f = E(x) \mid x \in X\}$ and uses their cluster assignments as pseudo-labels to subsequently supervise the update of E . The process starts with a randomly-initialized E and then iterates between clustering features generated by E and discriminative train-

ing to improve E using the clustering assignments. We note that, during training, only the weights of the classification ℓ_c -layer is reset between clustering iterations when the supervision-taxonomy or task is switched. DeepCluster uses a 2D CNN (*e.g.* ResNet-50) as its image encoder E and clusters the features after each epoch using k -means. We refer to the DeepCluster baseline in our paper as **Single-Modality Deep Clustering (SDC)**.

3.2. Multi-Modal Deep Clustering

Contrary to the single-modality case, there exist multiple encoders in a multi-modal setting, each of which encodes a different modality of the input. In our paper, we consider two modalities, the visual and the audio modalities from the unlabeled training video clips. In particular, let X be the set of unlabeled video clips, and E_v and E_a be the visual and audio encoders, respectively. Let $F_v = \{f_v = E_v(x) \in \mathbb{R}^{d_v} \mid x \in X\}$ and $F_a = \{f_a = E_a(x) \in \mathbb{R}^{d_a} \mid x \in X\}$ be the set of visual and audio deep features, respectively, produced by the two encoders. There are different ways we can adapt the deep clustering framework to a multi-modal input. We describe three approaches (MDC, CDC, and XDC) by detailing the steps taken at each deep clustering iteration.

Multi-Head Deep Clustering (MDC). This model builds on SDC by adding a second classification head supervised by the other modality. Thus, in this model, each encoder has two classification heads. At each deep clustering iteration, MDC uses the cluster assignments of F_v as pseudo-labels for one head and that of F_a as pseudo-labels for the other

head. Thus, each encoder needs to predict the cluster assignments of its own modality (as in SDC), but also those generated by the other modality.

Concatenation Deep Clustering (CDC). This model performs clustering of joint visual and audio features. Specifically, at each deep clustering iteration, CDC clusters vectors obtained by concatenating the visual and audio feature vectors, separately l_2 -normalized. Then, it uses the resulting cluster assignments as pseudo-labels to update the weights of both E_v and E_a .

Cross-Modal Deep Clustering (XDC). Each encoder in this model relies exclusively on the clusters learned from the other modality as the supervisory signal. At each deep clustering iteration, XDC clusters the audio deep features, F_a , and uses their cluster assignments as pseudo-labels to train the visual encoder, E_v . Vice versa, XDC uses cluster assignments of F_v as pseudo-labels to supervise E_a .

3.3. Optimization Challenges

In this subsection, we give the details of the full optimization cycle and discuss differences between the single-modality baseline and our multi-modal models.

Trivial solutions. As discussed in [5], the SDC baseline may converge to trivial solutions, corresponding to empty clusters or parameterizations of the encoder where the classifier predicts the same label regardless of the input. DeepCluster proposes workarounds to tackle these issues, involving reassigning empty cluster centers and sampling training images uniformly over the cluster assignments. While these strategies mitigate the issues, they do not fix the main cause of the problem, which is that SDC learns a discriminative classifier on the *same* input from which it learns the labels. On the other hand, our multi-modal deep clustering models are less prone to trivial solutions because they learn the discriminative classifier on one modality and obtain the labels from a *different* modality. In our training, we never encountered the issue of empty clusters or few-class predictions for any of our three multi-modal clustering approaches.

Initialization and convergence. Our initial pseudo-labels come from clustering features of randomly-initialized encoders. Such pseudo-labels are “good enough” to capture some weak similarities between the input samples as features from randomly-weighted networks have shown decent results on image and audio classification [50, 56]. Another potential option involves generating the initial pseudo-labels by clustering hand-crafted features, *e.g.* iDT [67] and audio spectrograms. Hand-crafted features capture low-level semantics that may help the encoders learn better or faster. Indeed, in small-scale experiments we observed that clustering handcrafted features in the initial iteration reduces the number of clustering iterations needed to learn a well-performing encoder. However, we decided to not pursue this further, since these features are computationally

expensive to extract and thus are not suitable for large-scale training on millions of examples. Furthermore, handcrafted features may bias the learning to reflect the design choices behind these manually-engineered descriptors.

Clustering and optimization schedule. Following previous work [5], we cluster the deep features using the k -means algorithm primarily because of its desirable properties of efficiency and scalability. The number of k -means clusters is a key hyperparameter in our framework. Intuitively, using more clusters makes the pretext task harder as it increases the number of pseudo-classes the classifier must recognize. On the other hand, the diversity of samples to cluster effectively dictates the maximum k for which the grouping is still sensible. Taking into account these factors, we explore the effects of k in our ablation study in Subsection 4.2. Another important hyperparameter of our framework is the number of training epochs for the encoders, before re-clustering the learned features. DeepCluster re-clusters after each epoch, which is an expensive design choice when scaling to millions of training samples. Thus, we choose to fix the pseudo-labels and train the encoders until the validation loss for predicting the pseudo-labels saturates. Then, we re-cluster the newly learned features, reassign pseudo-labels, reset the classification layer, and repeat the same process. We find this strategy more efficient, as it reduces the number of times we need to invoke k -means.

4. Experiments

4.1. Experimental Setup

Pretraining datasets. We use three large video datasets for our self-supervised pretraining: Kinetics [27], AudioSet [10], and IG65M [12]. It is worth noting that our approach is self-supervised, thus the labels from these datasets were **not used** during pretraining. While Kinetics and AudioSet are supervised benchmarks for action recognition and audio classification, IG65M is a large-scale weakly-supervised dataset collected from a social media website. The videos in Kinetics and AudioSet are about 10-second long, while the ones from IG65M last from 1 to 60 seconds. We use the training splits of these datasets for pretraining. These training sets include 240K, 2M, and 65M videos for Kinetics, AudioSet, and IG65M, respectively. We filter out around 7K Kinetics videos ($< 3\%$) that have no audio. Furthermore, we randomly sample 240K videos from AudioSet and denote this subset as AudioSet-240K. We generate this subset to have an AudioSet data of the same size as Kinetics, in order to study the effects of pretraining with the same data size but on a different data distribution and domain.

Downstream datasets. We evaluate our pretraining performance on three downstream benchmarks, UCF101 [58], HMDB51 [30], and ESC50 [49]. UCF101 and HMDB51 are video benchmarks for human action recognition, while

ESC50 is an environmental sound classification dataset. UCF101 contains about 13K videos from 101 human action classes, and HMDB51 consists of 7K clips spanning 51 different human activities. ESC50 has 2K clips of 50 different audio classes. UCF101 and HMDB51 have 3 official train/test splits, while ESC50 has 5 splits. We conduct our ablation study (Subsection 4.2) using split-1 of each dataset. We also report our average performance over all splits when we compare with state-of-the-art methods in Section 6.

Baselines. We compare our method against two baselines: **Scratch** and **Supervised Pretraining (Superv)**. The first baseline is a randomly-initialized model trained from scratch directly on the downstream task, while the second is a model pretrained in a supervised fashion on a large labeled dataset (*e.g.* Kinetics) and then finetuned on the downstream task. We note that these two baselines are commonly regarded as the lower and upper bounds to gauge the quality of self-supervised representation learning methods [1, 29].

Backbone architectures. We employ R(2+1)D [62] and ResNet [19] as our visual encoder E_v and audio encoder E_a , respectively. The input to E_v is a video clip of size $3 \times L \times H \times W$, where 3 refers to the RGB channels, L is the number of frames, and H and W are the frame height and width. The input to E_a is a spectrogram image of size $Q \times P$ extracted from the audio signal, where Q is the number of MEL filters and P is the number of temporal audio frames.

Pretraining and evaluation details. We choose the 18-layer variants of R(2+1)D and ResNet encoders. We use clips of $L = 8$ frames when pretraining and finetuning our visual encoder E_v . We scale frames such that the smallest dimension is 256 pixels and then random crop images of size 224×224 . We extract video clips at the original frame rate and employ temporal jittering when sampling training clips from the original video. For the audio input, we sample 2 seconds and use $Q = 40$ MEL filters and $P = 100$ audio frames. For inference on the downstream tasks, we uniformly sample 10 clips from each testing example and average their predictions to make a video-level prediction. We use only one crop per clip. More specifically, we use the center $8 \times 224 \times 224$ crop for video and the full 40×100 crop for audio. We provide more details on pretraining and finetuning parameters in the supplementary material.

4.2. Ablation Study

We present four studies in this subsection. The first study compares between the single-modality deep clustering baseline and the three multi-modal deep clustering models proposed in Section 3. The second one is conducted to understand the effects of the number of k -means clusters. The third study investigates the effects of pretraining data type and size. The final study compares the results of finetuning all layers vs. finetuning only the classifier layer. Finetuning is done on train split-1 and testing is done on the

Method	UCF101	HMDB51	ESC50
Scratch	54.5	24.1	54.3
Superv	90.9	58.0	82.3
SDC	61.8	31.4	66.5
MDC	68.4	37.1	70.3
CDC	<u>72.9</u>	<u>37.5</u>	<u>74.8</u>
XDC	74.2	39.0	78.0

Table 1: **Single-modality vs. multi-modal deep clustering.** We compare the four self-supervised deep clustering models (Section 3) and the two baselines, Scratch and Supervised Pretraining (Superv). The pretraining dataset is Kinetics, and the performance reported is the top-1 accuracy on split-1 of each downstream task. We can observe that all multi-modal models significantly outperform the single-modality deep clustering model. We mark in bold the best model and underline the second-best for each dataset.

Pretraining Dataset	Downstream Dataset	k				
		64	128	256	512	1024
Kinetics (240K videos)	UCF101	73.8	73.1	74.2	<u>74.0</u>	72.6
	HMDB51	36.5	39.0	<u>38.3</u>	37.7	37.7
	ESC50	78.0	<u>76.3</u>	75.0	74.5	71.5
AudioSet-240K (240K videos)	UCF101	77.4	<u>77.2</u>	76.7	77.1	75.3
	HMDB51	41.3	42.6	<u>41.6</u>	40.6	40.7
	ESC50	78.5	<u>77.8</u>	77.3	76.8	73.5
AudioSet (2M videos)	UCF101	84.1	84.3	84.9	<u>84.4</u>	84.2
	HMDB51	47.4	47.6	48.8	<u>48.5</u>	48.4
	ESC50	84.8	85.8	<u>85.0</u>	84.5	83.0

Table 2: **The number of clusters (k).** We show the effect of the number of k -means clusters on the performance of our XDC model. We show results when XDC is pretrained with self-supervision on three large datasets, and then finetuned with full supervision on three medium-size downstream datasets. The performance reported is the top-1 accuracy on split-1 of each downstream task. We can observe that the best k value increases as the size of the pretraining dataset increases.

test split-1 of these three benchmarks.

Study 1: Single-modality vs. multi-modal deep clustering. Our aim for this experiment is to compare the four models presented in Section 3. We pretrain SDC, MDC, CDC, and XDC on Kinetics and show their performance on the downstream tasks in Table 1. **Observations: (I)** The four self-supervised deep clustering models outperform the Scratch baseline on all downstream benchmarks. This shows that our self-supervised pretraining is effective and generalizes well to multiple tasks. **(II)** All multi-modal models (MDC, CDC, and XDC) significantly outperform SDC by up to 12.4%, 7.6%, and 11.5% on UCF101, HMDB51, and ESC50, respectively. This validates the importance of multi-modal modeling compared to single-modality. **(III)** XDC shows the best performance across all tasks. What distinguishes XDC from the other three models is that each modality encoder in XDC is self-supervised purely by the signal from the other modality. The encoders in CDC, MDC, and SDC all employ a self-supervision sig-

Method	Pretraining		Downstream Dataset		
	Dataset	Size	UCF101	HMDB51	ESC50
Scratch	None	0	54.5	24.1	54.3
Superv	ImageNet	1.2M	79.9	44.5	NA
Superv	Kinetics	240K	90.9	58.0	82.3
Superv	AudioSet-240K	240K	76.6	40.8	78.3
Superv	AudioSet	2M	84.0	53.5	90.3
XDC	Kinetics	240K	74.2	39.0	78.0
XDC	AudioSet-240K	240K	77.4	42.6	78.5
XDC	AudioSet	2M	84.9	48.8	<u>85.8</u>
XDC	IG65M	65M	91.5	63.1	84.8

Table 3: **Pretraining data type and size.** We compare XDC pretrained on four datasets vs. supervised pretrained (Superv) baseline models. The performance reported is the top-1 accuracy on split-1 of each downstream task. XDC performance improves as we increase the pretraining data size. XDC significantly outperforms fully-supervised pretraining on HMDB51 and UCF101.

nal coming from the same modality. Thus, this suggests that encoders learn better when purely supervised by a different modality. Overall, we find from this study that XDC performs the best among the three multi-modal approaches, so we opt to use XDC in the rest of the experiments.

Study 2: The number of k -means clusters. This study explores the effects of changing the hyperparameter k in k -means clustering. We pretrain XDC on three datasets, Kinetics, AudioSet-240K, and AudioSet, using $k = 64, 128, 256, 512,$ and 1024 clusters. Table 2 shows the effects of k on the downstream tasks. **Observations: (I)** the best value for k is not sensitive to the number of semantic labels in the downstream datasets, For example, although HMDB51 and ESC50 have about the same number of labels, they do not share the same best k value. **(II)** Similarly, the best value for k seems uncorrelated with the number of original semantic labels of the pretraining dataset, *e.g.* 400 in Kinetics. We reiterate here that our approach is self-supervised and **does not use** the labels of the pretraining dataset. **(III)** The best value for k tends to get larger as we increase the pretraining data size. For example, the best k for HMDB51 shifts from 128 to 256 when moving from pretraining on AudioSet-240K to the full AudioSet. We hypothesize that there is a more diverse sample set to cluster when the pretraining data size increases. Thus, we can have more fine-grained clusters (increase k) and make our self-supervised classification problem harder. This aligns with previous self-supervised learning works [15, 29] that showed benefits from making the pretext task harder. Given this observation, we opt to use $k = 2048$ for our large-scale pretraining experiments using 65 million unlabeled videos.

Study 3: Pretraining data type and size. Here, we present an experiment to investigate the effects of two pretraining characteristics, data size and type. To this end, we pretrain XDC on Kinetics (240K examples), AudioSet-240K

Method	Pretraining Dataset	UCF101		HMDB51		ESC50	
		f _c	all	f _c	all	f _c	all
Random	None	6.0±1.0	54.5	7.5±0.6	24.1	61.3±2.5	54.3
Superv	ImageNet	74.5	79.9	42.8	44.5	NA	NA
Superv	Kinetics	89.7	90.9	61.5	58.0	79.5	82.3
Superv	AudioSet	80.2	84.0	51.6	53.5	88.5	90.3
XDC	IG65M	<u>85.3</u>	91.5	<u>56.0</u>	63.1	<u>84.3</u>	84.8

Table 4: **Full finetuning vs. learning f_c-only.** We compare XDC against the supervised pretrained models (Superv) under two transfer-learning schemes: when models are used as features extractor (‘f_c’ column) and as a finetuning initialization (‘all’ column) for the downstream tasks. XDC fixed features outperform several fully-finetuned supervised models.

(240K examples), AudioSet (2M examples), and IG65M (65M examples). Kinetics and IG65M videos are collected originally for activity recognition, while AudioSet contains videos aimed for audio event classification. Besides the video datasets, we also experiment with ImageNet supervised pretraining. Since ImageNet is an image dataset, we inflate the images into static video clips (repeating the same frame) and pretrain our video model on this dataset. This will help us understand how much action recognition benefits from supervised pretraining on object classification. Table 3 presents the results of XDC self-supervised pretraining with different data types and sizes, and compares it to fully-supervised pretraining on ImageNet, Kinetics, and AudioSet. **Observations: (I)** XDC performance improves across all three downstream tasks, as the pretraining data size increases. For example, XDC performance on HMDB51 improves by 9.8% and 24.1% when pretrained on AudioSet and IG65M, respectively, compared to the results when pretrained on Kinetics. **(II)** XDC outperforms fully-supervised pretraining by 5.1% on HMDB51 and by 0.6% on UCF101. *To the best of our knowledge, XDC is the first method to demonstrate that self-supervision can outperform large-scale full-supervision in representation learning for action recognition.* **(III)** The performance of the fully-supervised pretrained model is influenced by the taxonomy of the pretraining data more than the size. For example, supervised-pretraining on Kinetics gives better performance on both UCF101 and HMDB51 compared to supervised-pretraining on AudioSet (which is more than 8 times larger than Kinetics) and ImageNet. On the other hand, XDC performance is less sensitive to the data type, as it implicitly learns the label space rather than depend on a space manually defined by annotators.

Study 4: Full finetuning vs. learning f_c-only. In this experiment, we study two approaches for transferring XDC to downstream tasks. *Full finetuning:* we finetune all parameters of the pretrained encoder on the downstream task. *Learning f_c-only:* we fix the pretrained encoder and learn a linear classifier for the downstream task, *i.e.*

a fully-connected (f_c) layer on top of the frozen features. Table 4 compares the performance of XDC with the supervised pretrained approaches under these two transfer-learning schemes. **Observations: (I)** The accuracy of most pretrained models (fully-supervised or self-supervised) degrades, when used as a fixed feature extractor compared to when they are fully-finetuned on the downstream tasks. Nonetheless, the relative performance of XDC compared to supervised pretrained models stays generally the same when fully vs. f_c -only finetuned on the downstream task. This suggests that XDC pretraining is useful both as a fixed feature extractor and as a pretraining initialization. **(II)** The performance of XDC as a fixed feature extractor exceeds the results of many fully-finetuned supervised models. For example, f_c -only XDC outperforms, by significant margins, the fully-finetuned supervised AudioSet and ImageNet-pretrained models on both UCF101 and HMDB51. **(III)** We observe that fully-supervised pretraining, followed by f_c -only finetuning performs well when the pretraining latent space (taxonomy) is well aligned with the downstream task. For example, pretraining on Kinetics with learning f_c -only on HMDB51 and UCF101 gives the best performance. This is expected as the label space of HMDB51 and UCF101 overlap largely with that of Kinetics. This observation suggests that fully-supervised pretraining is more taxonomy/downstream-task dependent, while our self-supervised XDC is taxonomy-independent.

5. Understanding XDC

“What does XDC actually learn? What semantic signals does the algorithm use to train its encoders?” Here, we try to answer these questions by inspecting the k -means clustering results produced by the last iteration of XDC.

XDC Clusters. Table 5 and Table 6 list the most common Kinetics concepts of some audio and video clusters, respectively, learned by XDC when trained on Kinetics. The clusters presented in these tables are the top and bottom clusters ranked by purity with respect to Kinetics action labels. We observe that the top-purity clusters learned from both modalities exhibit strong semantic coherence. For example, the audio 1st and 8-th ranked clusters (Table 5) include concepts relating to playing musical instruments that have similar sounds, while the 1st ranked video cluster (Table 6) also groups playing-instrument concepts, but mainly because of their appearance, as the cluster is all about guitars. Other interesting clusters include: grouping by motor-engine sounds (audio #10), by different swimming strokes (video #4), by different golf shots (video #5), and different cooking activities (video #10). In the bottom-ranked clusters, although the purity w.r.t. Kinetics concepts is low, we still find some coherence, mostly at the scene level: a farm setting in audio #127 (“grooming horse”, “milking cow”), or gym activities in video #63 (“pull ups”, “gymnastics tumbling”, “punch-

#	Kinetics concepts
1	play bagpipes(0.70), play harmonica(0.04), play violin(0.03)
2	scuba diving(0.33), snorkeling(0.27), feeding fish(0.11)
4	pass football(0.17), play kickball(0.06), catch/throw softball(0.05)
8	play cello(0.15), play trombone(0.11), play accordion(0.09)
10	mowing lawn(0.14), driving tractor(0.09), motorcycling(0.06)
127	abseiling(0.01), grooming horse(0.01), milking cow(0.01)
128	washing feet(0.01), motorcycling(0.01), headbanging(0.01)

Table 5: **XDC audio clusters.** Top and bottom XDC audio clusters ranked by clustering purity w.r.t. Kinetics labels. For each, we list the 3 concepts with the highest purity (given in parentheses).

#	Kinetics concepts
1	playing bass guitar(0.37), playing guitar(0.16), tapping guitar(0.15)
4	swim backstroke(0.21), swim breast stroke(0.16), swim butterfly stroke(0.10)
5	golf putting(0.18), golf chipping(0.11), golf driving(0.05)
9	windsurfing(0.12), jetskiing(0.10), water skiing(0.09)
10	cooking chicken(0.11), barbequing(0.07), frying vegetables(0.06)
63	pull ups(0.01), gymnastics tumbling(0.01), punching bag(0.01)
64	capoeira(0.01), riding elephant(0.01), feeding goats(0.01)

Table 6: **XDC video clusters.** Top and bottom XDC video clusters ranked by clustering purity w.r.t. Kinetics labels. For each, we list the 3 concepts with the highest purity (given in parentheses).

ing bag”). Many other bottom-ranked clusters appear to lack semantic coherence when viewed through the lens of Kinetics labels. However, one of the motivations behind the design of self-supervised methods is precisely to bypass the hand-design of label spaces, which may not be the optimal ones for general representation learning. Our experiments suggest that the label space learned by XDC yields strong and general audio and video features even though it does not align perfectly with the ontologies of existing datasets.

XDC Filters. Figure 2 visualizes and compares `conv_1` spatial and temporal filters of R(2+1)D learned by self-supervised XDC pretraining on IG65M versus fully-supervised pretraining on Kinetics. We observe some differences in both spatial and temporal filters between XDC and fully-supervised pretraining. In particular, XDC learns a more diverse set of motion filters.

6. State-of-the-Art Self-Supervised Learning Comparison

Here, we compare XDC with state-of-the-art self-supervised methods on action recognition in UCF101 [58] and HMDB51 [30], and on audio event classification in ESC50 [49] and DCASE [60]. We report top-1 accuracy averaged over all splits of these benchmarks.

Experimental setup. We use our XDC models pretrained on Kinetics, AudioSet, and IG56M. We do not modify the audio encoder pretraining. However, we re-train the XDC video encoder on the last clustering assignment using 32-frame clips instead, since most of state-of-the-art meth-

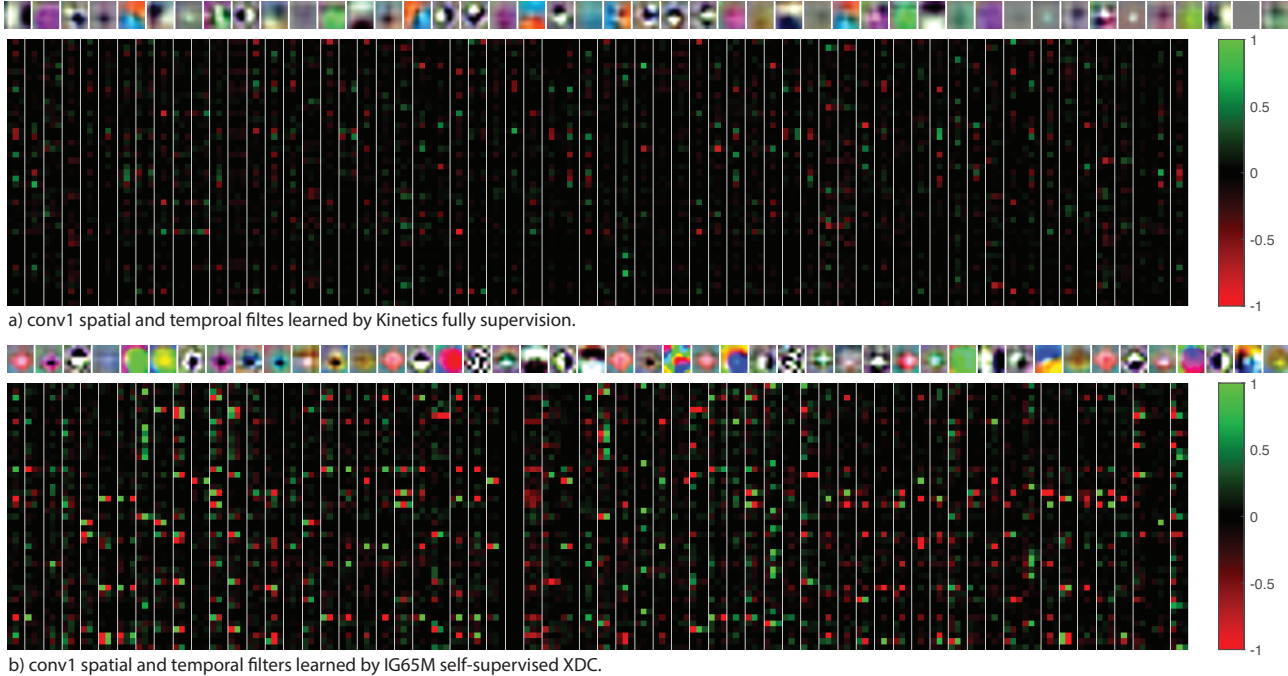


Figure 2: **R(2+1)D filters learned with self-supervised XDC vs. fully-supervised training.** (a) R(2+1)D `conv_1` filters learned by fully-supervised training on Kinetics. (b) The same filters learned by self-supervised XDC pretraining on IG65M. XDC learns a more diverse set of temporal filters compared to fully-supervised pretraining.

ods, both fully-supervised [62] and self-supervised [29], use longer clips. Similarly, we finetune on the action recognition downstream tasks using 32-frame clips for both XDC and the fully-supervised pretraining baselines. Inference is similar to our ablation experiments except for using 32-frame clips. For DCASE, following [29] we extract `conv_5` features for 60 uniformly-sampled clips from each audio sample and use a linear SVM on these features.

Video action recognition. Table 7 compares XDC pretrained on three large-scale datasets against state-of-the-art self-supervised methods, after finetuning on the UCF101 and HMDB51 benchmarks. We also compare against two fully-supervised methods pretrained on ImageNet and Kinetics and then finetuned on UCF101 and HMDB51. **Results:** (I) XDC pretrained on IG65M significantly outperforms fully-supervised pretraining on Kinetics: by 3.8% on HMDB51 and by 1.1% on UCF101. To the best of our knowledge, XDC is the first method to demonstrate that self-supervision can outperform large-scale full-supervision in representation learning for action recognition. (II) XDC pretrained on IG65M sets new state-of-the-art performance for self-supervised methods on both datasets, as it outperforms the current state-of-the-art self-supervised method AVTS [29] by 5.8% on HMDB51 and 5.2% on UCF101. (III) When constrained to the same pretraining dataset (AudioSet), XDC outperforms AVTS by 2.2% on UCF101 and is only slightly worse than AVTS on HMDB51 (by 0.6%).

Method	Pretraining		Evaluation	
	Architecture	Dataset	UCF	HMDB
Fully supervised	R(2+1)D-18	ImageNet	82.8	46.7
Fully supervised	R(2+1)D-18	Kinetics	93.1	63.6
Misra <i>et al.</i> [38]	CaffeNet	UCF/HMDB	50.2	18.1
Büchler <i>et al.</i> [3]	CaffeNet	UCF/HMDB	58.6	25.0
OPN [34]	VGG	UCF/HMDB	59.8	23.8
MotionPred [68]	C3D	Kinetics	61.2	33.4
RotNet3D [25]	3D-ResNet18	Kinetics	62.9	33.7
ST-Puzzle [28]	3D-ResNet18	Kinetics	65.8	33.7
ClipOrder [73]	R(2+1)D-18	Kinetics	72.4	30.9
DPC [18]	3D-ResNet34	Kinetics	75.7	35.7
L^3 -Net [1]	VGG	AudioSet	72.3	40.2
AVTS [29]	MC3-18	AudioSet	89.0	61.6
XDC (ours)	R(2+1)D-18	Kinetics	84.2	47.1
XDC (ours)	R(2+1)D-18	AudioSet	91.2	61.0
XDC (ours)	R(2+1)D-18	IG65M	94.2	67.4

Table 7: **State-of-the-art on video action recognition.** Comparison between XDC with self-supervised and fully-supervised methods on UCF101 and HMDB51 benchmarks. We report the average top-1 accuracy over the official splits. Not only does XDC set new state-of-the-art performance for self-supervised methods, it also outperforms fully-supervised Kinetics and ImageNet pretraining.

Similarly, XDC pretrained on Kinetics outperforms other Kinetics self-supervised pretrained methods [18] by 8.5% and 11.4% on UCF101 and HMDB51, respectively.

Audio event classification. Table 8 compares XDC

Method	Accuracy	Method	Accuracy
Autoencoder [2]	39.9	RG [51]	69
Random Forest [49]	44.3	LTT [35]	72
Piczak ConvNet [48]	64.5	RNH [53]	77
SoundNet [2]	74.2	Ensemble [61]	78
L^3 -Net [1]	79.3	SoundNet [2]	88
AVTS [29]	82.3	L^3 -Net [1]	<u>93</u>
ConvRBM [55]	86.5	AVTS [29]	94
XDC (AudioSet)	<u>84.8</u>	XDC (AudioSet)	<u>93</u>

(a) ESC50

(b) DCASE

Table 8: **State-of-the-art on audio event classification.** We compare XDC with self-supervised methods on ESC50 and DCASE benchmarks. We report the average top-1 accuracy over the official splits. XDC shows competitive performance.

pretrained on AudioSet with the state-of-the-art in self-supervised methods for audio. XDC achieves competitive results with only a 1.7% gap separating it from the state-of-the-art [55] on ESC50 and a 1% gap with the result of [29] on DCASE.

7. Conclusion

We have presented Cross-Modal Deep Clustering (XDC), a novel self-supervised learning method for video and audio. Our experiments showed that XDC outperforms not only existing self-supervised representation learning methods but also fully-supervised ImageNet- and Kinetics-pretrained models in action recognition. To the best of our knowledge, XDC is the first method to demonstrate self-supervision outperforming large-scale full-supervision in representation learning for action recognition.

References

- [1] Relja Arandjelovic and Andrew Zisserman. Look, listen and learn. In *ICCV*, 2017. 2, 5, 8, 9
- [2] Yusuf Aytar, Carl Vondrick, and Antonio Torralba. Soundnet: Learning sound representations from unlabeled video. In *NeurIPS*, 2016. 2, 9
- [3] Uta Büchler, Biagio Brattoli, and Björn Ommer. Improving spatiotemporal self-supervision by deep reinforcement learning. In *ECCV*, 2018. 8
- [4] Fabian Caba Heilbron, Victor Escorcia, Bernard Ghanem, and Juan Carlos Niebles. Activitynet: A large-scale video benchmark for human activity understanding. In *CVPR*, 2015. 1
- [5] Mathilde Caron, Piotr Bojanowski, Armand Joulin, and Matthijs Douze. Deep clustering for unsupervised learning of visual features. In *ECCV*, 2018. 2, 3, 4
- [6] Guillem Collell Talleda and Marie-Francine Moens. Is an image worth more than a thousand words? on the fine-grain semantic differences between visual and linguistic representations. In *COLING*, 2016. 2
- [7] Dima Damen, Hazel Doughty, Giovanni Maria Farinella, Sanja Fidler, Antonino Furnari, Evangelos Kazakos, Davide Moltisanti, Jonathan Munro, Toby Perrett, Will Price, and Michael Wray. Scaling egocentric vision: The epic-kitchens dataset. In *ECCV*, 2018. 1
- [8] Carl Doersch, Abhinav Gupta, and Alexei A Efros. Unsupervised visual representation learning by context prediction. In *ICCV*, 2015. 2
- [9] Basura Fernando, Hakan Bilen, Efstratios Gavves, and Stephen Gould. Self-supervised video representation learning with odd-one-out networks. In *CVPR*, 2017. 2
- [10] Jort F. Gemmeke, Daniel P. W. Ellis, Dylan Freedman, Aren Jansen, Wade Lawrence, R. Channing Moore, Manoj Plakal, and Marvin Ritter. Audio set: An ontology and human-labeled dataset for audio events. In *ICASSP*, 2017. 4, 12
- [11] A Gentile and S DiFrancesca. Academic achievement test performance of hearing-impaired students. united states, spring, 1969.(series d, no. 1). washington, dc: Gallaudet university. *Center for Assessment and Demographic Studies*, 1969. 1
- [12] Deepti Ghadiyaram, Matt Feiszli, Du Tran, Xueting Yan, Heng Wang, and Dhruv Mahajan. Large-scale weakly-supervised pre-training for video action recognition. In *CVPR*, 2019. 4, 12
- [13] Spyros Gidaris, Praveer Singh, and Nikos Komodakis. Unsupervised representation learning by predicting image rotations. *ICLR*, 2018. 2
- [14] Priya Goyal, Piotr Dollár, Ross Girshick, Pieter Noordhuis, Lukasz Wesolowski, Aapo Kyrola, Andrew Tulloch, Yangqing Jia, and Kaiming He. Accurate, large mini-batch SGD: training imagenet in 1 hour. *arXiv preprint arXiv:1706.02677*, 2017. 12
- [15] Priya Goyal, Dhruv Mahajan, Abhinav Gupta, and Ishan Misra. Scaling and benchmarking self-supervised visual representation learning. In *ICCV*, 2019. 6
- [16] Raghav Goyal, Samira Ebrahimi Kahou, Vincent Michalski, Joanna Materzynska, Susanne Westphal, Heuna Kim, Valentin Haenel, Ingo Fruend, Peter Yianilos, Moritz Mueller-Freitag, et al. The "something something" video database for learning and evaluating visual common sense. In *ICCV*, 2017. 1
- [17] Saurabh Gupta, Judy Hoffman, and Jitendra Malik. Cross modal distillation for supervision transfer. In *CVPR*, 2016. 2
- [18] Tengda Han, Weidi Xie, and Andrew Zisserman. Video representation learning by dense predictive coding. *arXiv preprint arXiv:1909.04656*, 2019. 8, 9
- [19] Kaiming He, Xiangyu Zhang, Shaoqing Ren, and Jian Sun. Deep residual learning for image recognition. In *CVPR*, 2016. 5
- [20] Rickye S. Heffner and Henry E. Heffner. *Evolution of Sound Localization in Mammals*, pages 691–715. Springer New York, New York, NY, 1992. 1
- [21] Geoffrey E Hinton, Simon Osindero, and Yee-Whye Teh. A fast learning algorithm for deep belief nets. *Neural computation*, 2006. 2
- [22] Geoffrey E Hinton and Ruslan R Salakhutdinov. Reducing the dimensionality of data with neural networks. *Science*, 2006. 2

- [23] Phillip Isola, Daniel Zoran, Dilip Krishnan, and Edward H Adelson. Learning visual groups from co-occurrences in space and time. *ICLR*, 2015. 2
- [24] Dinesh Jayaraman and Kristen Grauman. Slow and steady feature analysis: higher order temporal coherence in video. In *CVPR*, 2016. 2
- [25] Longlong Jing and Yingli Tian. Self-supervised spatiotemporal feature learning by video geometric transformations. *arXiv preprint arXiv:1811.11387*, 2018. 8
- [26] Andrej Karpathy, George Toderici, Sanketh Shetty, Thomas Leung, Rahul Sukthankar, and Li Fei-Fei. Large-scale video classification with convolutional neural networks. In *CVPR*, 2014. 1
- [27] Will Kay, Joao Carreira, Karen Simonyan, Brian Zhang, Chloe Hillier, Sudheendra Vijayanarasimhan, Fabio Viola, Tim Green, Trevor Back, Paul Natsev, Mustafa Suleyman, and Andrew Zisserman. The kinetics human action video dataset. *CoRR*, abs/1705.06950, 2017. 1, 4, 12
- [28] Dahun Kim, Donghyeon Cho, and In So Kweon. Self-supervised video representation learning with space-time cubic puzzles. In *AAAI*, 2019. 2, 8
- [29] Bruno Korbar, Du Tran, and Lorenzo Torresani. Cooperative learning of audio and video models from self-supervised synchronization. In *NeurIPS*, 2018. 2, 5, 6, 8, 9
- [30] H. Kuehne, H. Jhuang, E. Garrote, T. Poggio, and T. Serre. HMDB: a large video database for human motion recognition. In *ICCV*, 2011. 4, 7
- [31] Zihang Lai and Weidi Xie. Self-supervised learning for video correspondence flow. *BMVC*, 2019. 2
- [32] Quoc V Le, Will Y Zou, Serena Y Yeung, and Andrew Y Ng. Learning hierarchical invariant spatio-temporal features for action recognition with independent subspace analysis. In *CVPR*, 2011. 2
- [33] Honglak Lee, Alexis Battle, Rajat Raina, and Andrew Y Ng. Efficient sparse coding algorithms. In *NeurIPS*, 2007. 2
- [34] Hsin-Ying Lee, Jia-Bin Huang, Maneesh Singh, and Ming-Hsuan Yang. Unsupervised representation learning by sorting sequences. In *ICCV*, 2017. 2, 8
- [35] David Li, Jason Tam, and Derek Toub. Auditory scene classification using machine learning techniques. *AASP Challenge*, 2013. 9
- [36] William Lotter, Gabriel Kreiman, and David Cox. Deep predictive coding networks for video prediction and unsupervised learning. *ICLR*, 2017. 2
- [37] Michael Mathieu, Camille Couprie, and Yann LeCun. Deep multi-scale video prediction beyond mean square error. *ICLR*, 2016. 2
- [38] Ishan Misra, C Lawrence Zitnick, and Martial Hebert. Shuffle and learn: unsupervised learning using temporal order verification. In *ECCV*, 2016. 2, 8
- [39] Helmer R Myklebust. The psychology of deafness: Sensory deprivation, learning, and adjustment. 1960. 1
- [40] Jiquan Ngiam, Aditya Khosla, Mingyu Kim, Juhan Nam, Honglak Lee, and Andrew Y Ng. Multimodal deep learning. In *ICML*, 2011. 2
- [41] Mehdi Noroozi and Paolo Favaro. Unsupervised learning of visual representations by solving jigsaw puzzles. In *ECCV*, 2016. 2
- [42] Mehdi Noroozi, Hamed Pirsiavash, and Paolo Favaro. Representation learning by learning to count. In *ICCV*, 2017. 2
- [43] Risto Ntuen. *Attention and Brain Function*. 1992. 1
- [44] Andrew Owens and Alexei A Efros. Audio-visual scene analysis with self-supervised multisensory features. In *ECCV*, 2018. 2
- [45] Andrew Owens, Jiajun Wu, Josh H McDermott, William T Freeman, and Antonio Torralba. Ambient sound provides supervision for visual learning. In *ECCV*, 2016. 2
- [46] Deepak Pathak, Ross Girshick, Piotr Dollár, Trevor Darrell, and Bharath Hariharan. Learning features by watching objects move. In *CVPR*, 2017. 2
- [47] Deepak Pathak, Philipp Krahenbuhl, Jeff Donahue, Trevor Darrell, and Alexei A Efros. Context encoders: Feature learning by inpainting. In *CVPR*, 2016. 2
- [48] Karol J. Piczak. Environmental sound classification with convolutional neural networks. *MLSP*, 2015. 9
- [49] Karol J. Piczak. Esc: Dataset for environmental sound classification. In *ACM Multimedia*, 2015. 4, 7, 9
- [50] Jordi Pons and Xavier Serra. Randomly weighted cnns for (music) audio classification. In *ICASSP*, 2019. 4
- [51] Alain Rakotomamonjy and Gilles Gasso. Histogram of gradients of time-frequency representations for audio scene classification. *IEEE/ACM Trans. Audio, Speech and Lang. Proc.*, 2015. 9
- [52] Marc’auelio Ranzato, Fu Jie Huang, Y-Lan Boureau, and Yann LeCun. Unsupervised learning of invariant feature hierarchies with applications to object recognition. In *CVPR*, 2007. 2
- [53] Guido Roma, Waldo Nogueira, and Perfecto Herrera. Recurrence quantification analysis features for environmental sound recognition. *WASPAA*, 2013. 9
- [54] Andrew Rouditchenko, Hang Zhao, Chuang Gan, Josh McDermott, and Antonio Torralba. Self-supervised audio-visual co-segmentation. In *ICASSP*, 2019. 2
- [55] Hardik B. Sailor, Dharmesh M Agrawal, and Hemant A Patil. Unsupervised filterbank learning using convolutional restricted boltzmann machine for environmental sound classification. In *INTERSPEECH*, 2017. 9
- [56] Andrew M Saxe, Pang Wei Koh, Zhenghao Chen, Maneesh Bhand, Bipin Suresh, and Andrew Y Ng. On random weights and unsupervised feature learning. In *ICML*, 2011. 4
- [57] Ladan Shams and Robyn Kim. Crossmodal influences on visual perception. *Physics of Life Reviews*, 7(3):269–284, 2010. 1
- [58] Khurram Soomro, Amir Roshan Zamir, and Mubarak Shah. UCF101: A dataset of 101 human action classes from videos in the wild. In *CRCV-TR-12-01*, 2012. 4, 7
- [59] Nitish Srivastava, Elman Mansimov, and Ruslan Salakhudinov. Unsupervised learning of video representations using lstms. In *ICML*, 2015. 2
- [60] D. Stowell, D. Giannoulis, E. Benetos, M. Lagrange, and M. D. Plumbley. Detection and classification of acoustic scenes and events. *IEEE Transactions on Multimedia*, 17(10):1733–1746, Oct 2015. 7

- [61] Dan Stowell, Dimitrios Giannoulis, Emmanouil Benetos, Mathieu Lagrange, and Mark D. Plumbley. Detection and classification of acoustic scenes and events. *TM*, 2015. 9
- [62] Du Tran, Heng Wang, Lorenzo Torresani, Jamie Ray, Yann LeCun, and Manohar Paluri. A closer look at spatiotemporal convolutions for action recognition. In *CVPR*, 2018. 5, 8
- [63] Pascal Vincent, Hugo Larochelle, Yoshua Bengio, and Pierre-Antoine Manzagol. Extracting and composing robust features with denoising autoencoders. In *ICML*, 2008. 2
- [64] Carl Vondrick, Hamed Pirsiavash, and Antonio Torralba. Anticipating visual representations from unlabeled video. In *CVPR*, 2016. 2
- [65] Carl Vondrick, Hamed Pirsiavash, and Antonio Torralba. Generating videos with scene dynamics. In *NeurIPS*, 2016. 2
- [66] Carl Vondrick, Abhinav Shrivastava, Alireza Fathi, Sergio Guadarrama, and Kevin Murphy. Tracking emerges by coloring videos. In *ECCV*, 2018. 2
- [67] Heng Wang and Cordelia Schmid. Action recognition with improved trajectories. In *ICCV*, 2013. 4
- [68] Jiangliu Wang, Jianbo Jiao, Linchao Bao, Shengfeng He, Yunhui Liu, and Wei Liu. Self-supervised spatio-temporal representation learning for videos by predicting motion and appearance statistics. In *CVPR*, 2019. 2, 8
- [69] Xiaolong Wang and Abhinav Gupta. Unsupervised learning of visual representations using videos. In *ICCV*, 2015. 2
- [70] Xiaolong Wang, Allan Jabri, and Alexei A Efros. Learning correspondence from the cycle-consistency of time. In *CVPR*, 2019. 2
- [71] Xiaolong Wang, Allan Jabri, and Alexei A. Efros. Learning correspondence from the cycle-consistency of time. In *CVPR*, 2019. 2
- [72] Donglai Wei, Joseph J Lim, Andrew Zisserman, and William T Freeman. Learning and using the arrow of time. In *CVPR*, 2018. 2
- [73] Dejing Xu, Jun Xiao, Zhou Zhao, Jian Shao, Di Xie, and Yueting Zhuang. Self-supervised spatiotemporal learning via video clip order prediction. In *CVPR*, 2019. 2, 8
- [74] Richard Zhang, Phillip Isola, and Alexei A Efros. Colorful image colorization. In *ECCV*, 2016. 2
- [75] Hang Zhao, Chuang Gan, Andrew Rouditchenko, Carl Vondrick, Josh McDermott, and Antonio Torralba. The sound of pixels. In *ECCV*, 2018. 2

Supplementary Material

A. Additional qualitative results

XDC Clusters. Tables 13 and 14 present the top and bottom 10 audio and video clusters learned with XDC on Kinetics, ranked by their purity with respect to Kinetics labels. We list the 5 most frequent concepts of each cluster.

B. Hyperparameters and training details

Training. We train our models using caffe2 with distributed SGD on a GPU cluster, and employ the warmup scheme proposed in [14]. The main training parameters are presented in Table 9. We note that the epoch size can be different from the actual number of videos. This is because the total number of clips the model sees during training (with temporal jittering) can be larger than the number of videos.

Pretraining parameters. We pretrain XDC and other baselines using the parameters described in Table 10. Early stopping is used for pretraining on small datasets such as Kinetics [27] and AudioSet [10] to stop before the model starts overfitting on the pretext task. For IG65M [12], we do not observe overfitting. We pretrain XDC on IG65M longer in the last deep clustering iteration (denoted as IG65M* in Table 10). When pretraining our R(2+1)D on longer clips (*e.g.* 32 frames), due to the GPU memory limit, we reduce the mini-batch size to 8 (instead of 32) and the base learning rate to 0.0025 (instead of 0.01).

Finetuning parameters. We provide finetuning hyperparameters in Table 11. Different pretraining methods may have different optimal base learning rate when finetuned on downstream tasks. Thus to make a fair comparison, we cross-validate the finetuning using the same set of base learning rates (presented in Table 12) and report the best result for each pretraining method. As we observed that higher learning rates tend to be beneficial when learning FC-only, we use a wider set of learning rates to cross-validate FC-only models. As done during pretraining, when finetuning R(2+1)D on longer clips (*i.e.* 32 frames), we reduce the mini-batch size to 8 and reduce the base learning rate to 1/4 of its original rate.

Abv.	Name	Description
es	epoch size	The total number of examples the model trains on in one epoch.
bs	batch size	The size of a mini-batch.
lr	base lr	The initial learning rate.
we	warmup epoch	The number of epochs used for warmup [14].
se	step epoch	Every se epochs, the learning rate
γ	lr decay	is decayed by multiplying with γ .
te	total epoch	The training lasts for te epochs.
wd	weight decay	The weight decay used in SGD.
e-stop	early stop	Stop training when validation loss is increased in 3 consecutive epochs.

Table 9: **Training parameter definitions.** The abbreviations and descriptions of each training parameters.

method	dataset	es	bs	lr	we/se/te	wd	e-stop
Superv	Kinetics	1M	32	0.01	10/10/45	10^{-4}	no
Superv	AudioSet	2M	32	0.04	10/20/45	10^{-5}	no
All DCs	Kinetics	1M	32	0.01	10/10/30	10^{-4}	yes
All DCs	AudioSet	2M	32	0.01	10/10/45	10^{-4}	yes
All DCs	IG65M	10M	32	0.01	1/3/10	10^{-4}	no
All DCs	IG65M*	10M	32	0.01	0/9/30	10^{-4}	no

Table 10: **Pretraining parameters.** We use early-stopping for Kinetics and AudioSet since we observe some overfitting on the pretext tasks. For the last iteration of XDC on IG65M, we pretrain XDC 3x longer (iteration denoted as IG65* in this table). γ is set to 0.01 for all settings.

dataset	es	bs	we/se/te	wd	e-stop
HMDB51	40K	32	2/2/8	0.005	no
UCF101	106K	32	2/2/8	0.005	no
ESC50	20K	32	2/2/8	0.005	no

Table 11: **Finetuning parameters.** Different pretraining methods have different ranges of optimal base learning rate when finetuning on downstream tasks. Thus, we cross-validate all methods with the same set of base learning rates and report the best result for each method. γ is set to 0.01 for all settings.

Setup	Base learning rates
Full	0.001, 0.002, 0.004, 0.006, 0.008, 0.01
FC only	0.001, 0.002, 0.004, 0.006, 0.008, 0.01, 0.02, 0.04

Table 12: **Finetuning base learning rates.** For a fair comparison, we cross-validate all pretraining methods with the same set of base learning rates. We report the best finetuning result for each method. Learning FC-only benefits from cross-validation with a wider range of base learning rates.

#	Kinetics concepts
1	playing bagpipes(0.70), playing 2harmonica(0.04), playing violin(0.03), playing accordion(0.02), marching(0.01)
2	scuba diving(0.33), snorkeling(0.27), feeding fish(0.11), canoeing or kayaking(0.02), jumping into pool(0.02)
3	playing cymbals(0.21), playing drums(0.17), marching(0.03), air drumming(0.02), drumming fingers(0.02)
4	passing American football(0.17), play kickball(0.06), catching or throwing softball(0.05), kick field goal(0.02), sled dog racing(0.02)
5	presenting weather forecast(0.17), playing poker(0.05), testifying(0.03), tying knot (not on a tie)(0.02), golf putting(0.02)
6	hurling (sport)(0.17), swimming backstroke(0.05), skiing slalom(0.04), vault(0.03), ski jumping(0.02)
7	presenting weather forecast(0.15), news anchoring(0.05), filling eyebrows(0.02), braiding hair(0.02), tossing salad(0.02)
8	playing cello(0.15), playing trombone(0.11), playing accordion(0.09), playing harp(0.07), playing clarinet(0.06)
9	playing recorder(0.14), playing violin(0.12), playing trumpet(0.08), playing harmonica(0.07), tapping guitar(0.06)
10	mowing lawn(0.14), driving tractor(0.09), motorcycling(0.06), blowing leaves(0.04), water skiing(0.04)
119	side kick(0.02), front raises(0.01), dunking basketball(0.01), smoking(0.01), high kick(0.01)
120	clay pottery making(0.02), crawling baby(0.02), brushing teeth(0.01), playing harmonica(0.01), eating spaghetti(0.01)
121	pushing cart(0.01), hula hooping(0.01), high kick(0.01), blowing out candles(0.01), bench pressing(0.01)
122	shot put(0.01), feeding birds(0.01), squat(0.01), push up(0.01), high jump(0.01)
123	opening present(0.01), petting cat(0.01), pushing cart(0.01), washing dishes(0.01), punching bag(0.01)
124	trimming or shaving beard(0.01), petting cat(0.01), front raises(0.01), massaging back(0.01), tai chi(0.01)
125	feeding birds(0.01), tobogganing(0.01), riding elephant(0.01), feeding goats(0.01), jumping into pool(0.01)
126	climbing tree(0.01), writing(0.01), archery(0.01), brushing hair(0.01), shining shoes(0.01)
127	abseiling(0.01), grooming horse(0.01), milking cow(0.01), feeding goats(0.01), juggling balls(0.01)
128	washing feet(0.01), motorcycling(0.01), headbanging(0.01), cheerleading(0.01), krumping(0.01)

Table 13: **XDC audio clusters.** Top and bottom 10 XDC audio clusters ranked by clustering purity w.r.t. Kinetics labels. For each, we list the 5 concepts with the highest purity (given in parentheses).

#	Kinetics concepts
1	playing bass guitar(0.37), playing guitar(0.16), tapping guitar(0.15), strumming guitar(0.09), playing ukulele(0.09)
2	scuba diving(0.36), snorkeling(0.32), feeding fish(0.10), diving cliff(0.02), jumping into pool(0.02)
3	presenting weather forecast(0.26), playing poker(0.10), news anchoring(0.05), testifying(0.03), giving or receiving award(0.02)
4	swimming backstroke(0.21), swimming breast stroke(0.16), swimming butterfly stroke(0.10), play ice hockey(0.04), jump into pool(0.04)
5	golf putting(0.18), golf chipping(0.11), golf driving(0.05), hitting baseball(0.03), archery(0.03)
6	hurling (sport)(0.17), passing American football (in game)(0.06), skiing slalom(0.04), playing ice hockey(0.03), vault(0.03)
7	filling eyebrows(0.13), braiding hair(0.05), massaging back(0.05), curling hair(0.05), dying hair(0.03)
8	playing cello(0.12), playing harp(0.12), playing trombone(0.06), playing piano(0.06), playing accordion(0.05)
9	windsurfing(0.12), jetskiing(0.10), water skiing(0.09), surfing water(0.08), kitesurfing(0.06)
10	cooking chicken(0.11), barbequing(0.07), frying vegetables(0.06), cooking sausages(0.04), making pizza(0.04)
55	yoga(0.02), folding napkins(0.02), doing nails(0.02), cutting watermelon(0.01), writing(0.01)
56	eating spaghetti(0.02), making pizza(0.02), brushing teeth(0.02), blowing out candles(0.02), reading book(0.02)
57	answering questions(0.02), tai chi(0.02), dancing ballet(0.02), dunking basketball(0.02), sign language interpreting(0.01)
58	trimming or shaving beard(0.02), barbequing(0.02), kissing(0.02), dining(0.01), playing poker(0.01)
59	punching bag(0.02), blowing out candles(0.02), pumping fist(0.02), dancing gangnam style(0.02), opening present(0.01)
60	feeding goats(0.02), blowing out candles(0.02), milking cow(0.02), arm wrestling(0.02), finger snapping(0.02)
61	air drumming(0.02), pumping fist(0.02), pushing cart(0.02), brushing teeth(0.02), eating ice cream(0.01)
62	clean and jerk(0.01), robot dancing(0.01), bench pressing(0.01), side kick(0.01), punching bag(0.01)
63	pull ups(0.01), gymnastics tumbling(0.01), punching bag(0.01), cracking neck(0.01), eating ice cream(0.01)
64	capoeira(0.01), riding elephant(0.01), feeding goats(0.01), feeding birds(0.01), crawling baby(0.01)

Table 14: **XDC video clusters.** Top and bottom 10 XDC video clusters ranked by clustering purity w.r.t. Kinetics labels. For each, we list the 5 concepts with the highest purity (given in parentheses).